

Shape instability, depinning, and creep motion of magnetic domain walls driven by electrical current

R. Díaz Pardo,¹ N. Moisan,¹ L. Albornoz,^{1,2,3} A. Lemaître,⁴ J. Curiale,^{2,3} and V. Jeudy^{1,*}

¹*Laboratoire de Physique des Solides, Université Paris-Sud,
Université Paris-Saclay, CNRS, UMR8502, 91405 Orsay, France.*

²*Instituto de Nanociencia y Nanotecnología CNEA-CONICET, Centro Atómico Bariloche,
Av. Bustillo 9500, R8402AGP, San Carlos de Bariloche, Argentina.*

³*Instituto Balseiro, Univ. Nac. Cuyo - CNEA, Av. Bustillo 9500,
R8402AGP, S. C. de Bariloche, Rio Negro, Argentina.*

⁴*Centre de Nanosciences et de Nanotechnologies (C2N), CNRS,
Univ. Paris-Sud, Université Paris-Saclay, 91120 Palaiseau, France.*

(Dated: May 17, 2022)

We explore the dynamics and self-affinity of magnetic domain wall driven by electrical current, in a ferromagnetic (Ga,Mn)(As,P) thin film with perpendicular magnetic anisotropy. We show that common universal behaviors corresponding to the so-called quenched Edwards-Wilkinson universality class are shared by current and magnetic field driven domain wall motion. The universal behaviors of the creep and depinning dynamical regimes can be described by a unique self-consistent model. However, the transverse orientation between current and domain wall is found to be unstable, leading to the formation of faceted structures typical of the quenched Kardar-Parisi-Zhang universality class.

PACS numbers: 75.78.Fg, 68.35.Rh, 64.60.Ht, 05.70.Ln, 47.54.-r

The displacement of small spin texture as magnetic domain walls (DWs) thanks to spin torque effects is at the basis of potential applications to magnetic memory storage [1]. An important effort is dedicated to search for magnetic materials [2, 3] with large and well controlled DW velocities. However, DWs are very sensitive to weak pinning defects [4, 5], which strongly reduce their mobility and produce roughening and stochastic avalanche-like motion [6, 7]. Therefore, it is particularly interesting to better understand the contribution of pinning to current induced DW dynamics.

Magnetic domain walls [4, 5, 8–12] present surprising universal critical behaviors, encountered in a wide variety of moving interfaces such as the reaction front propagation in disordered flows [13], growing bacterial colonies [14], wetting [15], motion of ferroelectric domain walls [16], to name a few. The displacement interfaces presents self-affine scaling variations: $u \sim L^\zeta$, where u is the position of interface, L a distance between two points of the interface and ζ the roughness exponent. Moreover, a depinning driving force f_d separates the so-called creep ($f < f_d$) and depinning ($f \gtrsim f_d$) regimes. In the creep regime, the velocity varies [4, 11, 17] as an Arrhenius law $v \sim e^{-\Delta E/k_B T}$, where $k_B T$ is the thermal fluctuation energy. ΔE is the effective pinning energy barriers height, which follows a universal power law variation with the drive $\Delta E \sim f^{-\mu}$, where μ is the creep exponent. In the depinning regime [12, 18, 19], the effective pinning barriers are collapsed. The velocity presents power law variations with drive f and temperature T : $v \sim (f - f_d)^\beta$ and $v(f_d) \sim T^\psi$, where β and ψ are the depinning and thermal rounding exponents, respectively.

Universal behaviors have been extensively investigated

for DWs driven by magnetic field ($f \propto H$) in ferromagnetic ultrathin films. For a large variety of materials, the measured values of the creep ($\mu = 1/4$) [4, 5, 9–11] and roughness ($\zeta \approx 0.66$ [4, 9] and $\zeta \approx 1.25$ [7]) exponents, are compatible with the prediction for the motion of an elastic 1D line in a short-range weak pinning disorder, described by the so-called quenched Edwards-Wilkinson (qEW) universality class with [20], and without [17, 21] anharmonic contributions, respectively. For the depinning transition, the compatibility predictions for the qEW universality class ($\beta = 0.25$ [18], and $\psi = 0.15$ [19]) was evidenced recently [12].

In contrast, the universal behaviors of DW motion induced by electric current are more contentious. To the best of our knowledge, the universality of depinning transition have not yet been explored. For the creep motion, a compatibility with $\mu = 1/4$ is suggested for DW driven by the conventional spin transfer torque (STT) in Pt/Co/Pt nanowires [22] and by spin orbit torque (SOT), in ferromagnets [2]. However, different values were reported for other materials ($\mu = 0.33 \pm 0.06$ for (Ga,Mn)As [8] and $\mu = 0.39 \pm 0.06$ for Ta/CoFeB/MgO [10]), which are difficult to interpret. Moreover, an important difference between magnetic field and current driven motion is reported in the literature. The current produces tilting and faceting [5, 23] of DWs. Those features could suggest a compatibility with the so-called quenched Kardar-Parisi-Zhang (qKPZ) universality class [5]. However, in the direction perpendicular to DW, the roughness is characterized by an exponent ($\zeta_j = 0.69 \pm 0.04$) independent of DW tilting angle and compatible the measurement obtained for field driven DW motion ($\zeta_H = 0.68 \pm 0.04$), while a different value ($\zeta_j = 0.99 \pm 0.01$) is obtained in

the direction of current. Therefore, whether distinct or common universality classes describe the motion of DWs driven by current and magnetic field remains an open question.

In this letter, we report a study of DW tilting and faceting process complemented by extensive investigations on the DW dynamics and self-affinity. Independent measurements of creep and roughness critical exponents reveal common universal behaviors of current and magnetic field driven DW motion, which are found to extend up to the depinning transition.

Experimental technique. The experiments were performed with rectangles of a 4 nm thick (Ga,Mn)(As,P)/(Ga,Mn)As bilayer film patterned by lithography. The film was grown on a (001) GaAs/AlAs buffer [24]. It has an effective perpendicular anisotropy and a Curie temperature (T_c) of 65 K. The sizes of rectangles were 133×210 , 228×302 , and $323 \times 399 \mu\text{m}^2$ (see supplemental material [25] for the details). Two 40 μm wide gold electrodes (separated by 110, 204, and 300 μm , respectively) were deposited by evaporation parallel to the narrow sides of rectangles [25], and were used to generate an homogeneous current density. The pulse amplitude varied between 0 and 11 GA/m². We verified that the Joule effect had a negligible contribution on DW dynamics [25]. Perpendicular magnetic field pulses of adjustable amplitude (0-65 mT) were produced by a 75 turns small coil (diameter ~ 1 mm) mounted on the sample. The set-up was placed in an optical He-flow cryostat allowing to stabilize the temperature between 5.7 K and T_c . The DW displacement is observed using a magneto-optical Kerr microscope (resolution $\sim 1 \mu\text{m}$). The DW velocity is defined as the ratio between the average displacement Δx and the pulse duration Δt [25], which varies between 1 μs and 120 s.

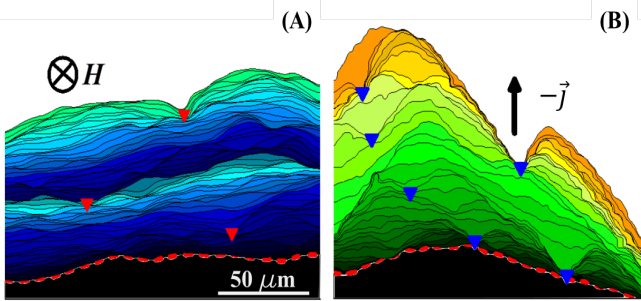


Figure 1. Time-evolution of DW shape. Successive positions of a DW, at $T = 28$ K, driven by (A) magnetic field ($H = 0.16$ mT, delay between images $\Delta t = 0.5$ s, total duration 60 s) and (B) current ($j = 0.45$ GA/m², $\Delta t = 0.5$ s, total duration 16 s), observed at the same sample location. The pictogram \otimes shows the direction of field. The DW move in the direction opposite to the current density, which is indicated by the arrow. The initial DW position is underlined by a thick dot line. The triangles indicate strongest DW pinning positions.

Evolution of DW shape. The time-evolution of an initially almost flat DW when driven by magnetic field and electrical current is compared in Fig. 1. For field driven DW motion, the average successive displacements are relatively similar. The initial DW shape is almost conserved during the motion. The DWs become sometimes strongly pinned and curved (see Fig. 1 (A)) but flattened again when depinned, due to the combined effects of DW elasticity and driving force, which acts as a pressure ($f \propto H$). In contrast, the initial DW shape is significantly altered by the current (see Fig. 1 (B)). DWs form faceted structures. There is a clear reduction of DW displacements with increasing tilting angle θ until DWs stop (on the experiment time scale) at a critical angle ($\theta_c = 55^\circ \pm 7^\circ$). The formation of faceted DWs suggests different universal behaviors for current- and field-driven DW motion [5, 20, 26].

Origin of domain wall faceting. In order to investigate the origin of DW faceting in details, we first analyze the evolution of an initially almost rectangular domain placed in a uniform current (see Fig. 2). As it can be observed, the side DWs, which are aligned along the current (i.e., $\vec{j} \perp \vec{n}$, where \vec{n} is the direction normal to DW) remain almost motionless. In contrast, the back and front DWs perpendicular to the current (i.e., $\vec{j} \parallel \vec{n}$) are significantly displaced. Surprisingly, the back DW moves faster than the front DW, which causes the collapse of the domain (see Fig. 2 (E-F)). Another interesting feature is the increasingly pointed shape of the front DW (not observed for the back DW). Here, the faceting of the front DW develops without any contribution of "strong" pinning sites observed in Fig. 1 (B), which suggests that the transverse orientation between DW and current is unstable.

To explore more quantitatively the contribution of different forces on the shape evolution of DWs, we measured systematically DW displacements Δx_n along the direction \vec{n} as a function of the angle θ between \vec{n} and $-\vec{j}$, for a fixed magnitude of current density and pulse duration Δt (see Fig. 2 (G and H)). As shown in Fig. 2 (I), Δx_n varies linearly with $\cos \theta$, and there is a critical angle θ_c for which $\Delta x_n \rightarrow 0$. This suggests a simple model describing DW displacement as a balance between driving f and pinning f_{pin} forces: $\Delta x_n \propto f - f_{pin}$. Assuming $f \propto -\vec{j} \cdot \vec{n}$ and a constant value for f_{pin} ($\propto j_{pin}$) leads to the relation $\Delta x_n \propto j(\cos \theta - \cos \theta_c)$, where the critical angle is defined by $\cos \theta_c = j_{pin}/j$. The rather good agreement between the model and experimental results shown in Fig. 2 (I) suggests that the DW faceting originates from the directionality of driving force ($f \propto -\vec{j} \cdot \vec{n}$), which tends to destabilize the transverse orientation of DWs with current and to reduce DW velocity, and a critical tilting angle θ_c determined by the ratio between magnitude of pinning and drive. Taking this into account, the different shape evolutions of the front and back DWs observed in Fig. 2 (A-F) can be interpreted as a result

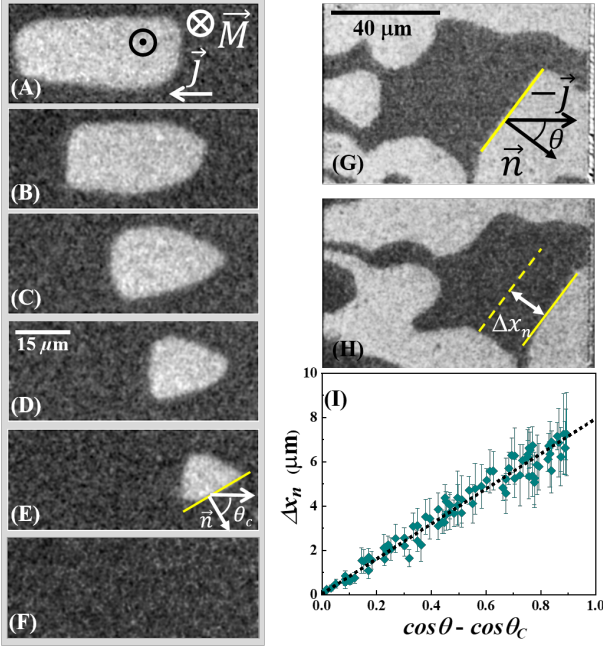


Figure 2. **Current driven domain wall motion** (A-F) Evolution of an almost rectangular magnetic domain submitted to pulses of current (duration $\Delta t = 6\mu\text{s}$ and amplitude $j = 11\text{ GA/m}^2$) for $T = 45\text{ K}$. The gray levels correspond to opposite directions of magnetization \vec{M} perpendicular to the sample. The back DW conserves its shape and velocity while the front DW becomes pointed, which reduces its velocity and leads to the collapse of the domain (see images E and F). (G-H) Two successive images of domains ($\Delta t = 1\mu\text{s}$ and $j = 11\text{ GA/m}^2$) showing, for $T = 55\text{ K}$, the displacement Δx_n of a tilted DW (see the dashed and solid segments) along its normal direction \vec{n} . θ is the tilting angle between \vec{n} and $-\vec{j}$. (I) Linear variation of Δx_n with $\cos\theta - \cos\theta_c$. No DW motion ($\Delta x_n = 0$) is observed for $\theta > \theta_c (= 84^\circ)$.

of opposite contributions of DW elasticity. The two side DWs pull the extremities of back (front) DWs in the $-\vec{j}$ (\vec{j}) direction, which tends to stabilize (destabilize) the transverse DW orientation.

DW dynamics and creep exponent. Let us now discuss of DW universal behaviors starting with investigations on current driven DW dynamics. In order to circumvent the variation of driving force with DW tilt, the velocity measurements presented later are all performed from almost flat DWs transverse to current ($\theta \approx 0$) as the initial states shown in Fig.1. The velocity curves are reported in Fig. 3 and show similar features to those usually encountered in the literature for magnetic field driven DW dynamics [9, 11, 12]. At low drive ($j < j_d$), the velocity follows a strong non-linear variation with drive and temperature, which characterizes the thermally activated creep regime (see the inset in Fig. 3). The curves present a change of curvature below and above the depinning threshold ($j = j_d$). The linear variation observed well above threshold corresponds to the flow regime. Here

the exploration of DW dynamics was limited to the temperature range $T = 49\text{--}59\text{ K}$, due to large thermal fluctuations impeding accurate displacement measurements above 59 K and to an increase of the depinning threshold beyond experimental access below 49 K .

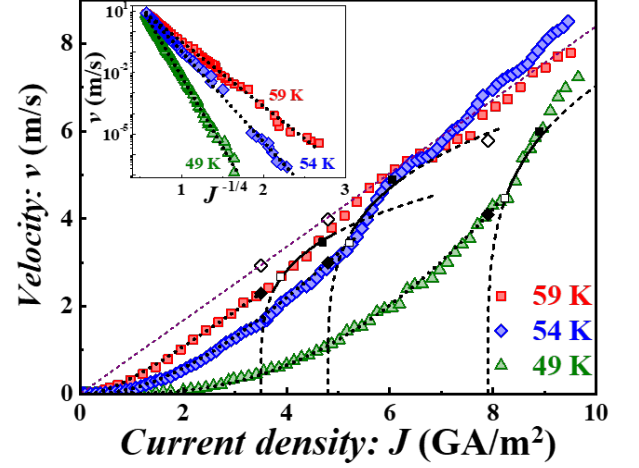


Figure 3. **Analysis of domain wall dynamics.** DW velocity versus current density j for different temperatures. The solid and empty diamonds correspond to $v(j_d)$, and $v_T(j_d)$, respectively. The dashed lines are fits of Eqs. 1 and the dotted line shows the linear dependence corresponding to the flow regime for $T = 59\text{ K}$. A sliding average over 5 points is used to smooth the curves. Inset: semi-log plot of the velocity versus $j^{-1/4}$ highlighting the thermally activated creep regime.

For more quantitative insights on universal behaviors of DW dynamics, we follow the analysis developed in Ref. [12] for magnetic field driven DW motion. The data were compared to the creep and depinning laws:

$$v(j) = \begin{cases} v(j_d) \exp(-\frac{\Delta E}{k_B T}) & \text{creep} \\ \frac{v_T(j_d)}{x_0} (\frac{j - j_d}{j_d})^\beta & \text{depinning,} \end{cases} \quad (1)$$

where $v(j_d)$ is the velocity at depinning threshold, and $v_T(j_d) = v(j_d)(T_d/T)^\psi$ the velocity that DW would reach at $j = j_d$ without pinning, i.e. within the flow regime. For the creep regime ($j < j_d$), the energy barrier height is given by $\Delta E = k_B T_d ((j/j_d)^{-\mu} - 1)$, where $k_B T_d$ is the characteristic height of effective pinning barrier. For the depinning regime ($j \gtrsim j_d$), Eq. 1 is only valid within the range: $j_d[1 + (0.8(T_d/T)^{-\psi})^{1/\beta}] < j < j_d[1 + (x_u(T_d/T)^{-\psi})^{1/\beta}]$, with $x_u = 1.2$ (see Ref. 12 for details). The depinning exponents are $\beta = 0.25$, and $\psi = 0.15$, and the critical parameter $x_0 = 0.65$ [12].

We performed a global fit of Eqs. 1 for all the temperatures. The exponent μ was set as a free shared parameter while the material and temperature dependent pinning parameters (j_d , v_T , and T_d) were taken as independent. As it can be observed in Fig. 3, the fits present a good agreement with the data. The same analysis was performed for magnetic field driven DW mo-

T	Current			Magnetic field		
	j_d	$v_T(j_d)$	T_d	H_d	$v_T(H_d)$	T_d
49	8.4 (0.6)	5.1 (0.5)	439 (35)	32.4 (0.4)	7.6 (0.4)	310 (10)
54	4.9 (0.4)	3.5 (0.4)	349 (25)	20.5 (0.4)	5.2 (0.2)	323 (20)
59	3.5 (0.3)	2.3 (0.2)	296 (30)	19.7 (0.5)	5.0 (0.4)	329 (12)

Table I. **Pinning parameters of DW dynamics.** Fitting parameters of Eqs. 1. *Units:* T and T_d are in Kelvin, v_T in m/s , j_d in GA/m^2 and, H_d in mT . For the fits of the velocity-field curves, see [25].

tion [25]. A comparison of the pinning parameters obtained in both cases is shown in Table I. The pretty close heights of effective pinning energy barrier ($k_B T_d$) reported for each temperature indicates that a similar weak pinning disorder control both dynamics. Moreover, the values of creep exponent obtained with field ($\mu_H = 0.247 \pm 0.011$) [25] and current ($\mu_j = 0.259 \pm 0.004$) match within experimental error bars [27]. A good agreement is also found with the self-description of the creep and depinning regimes, already proposed for magnetic field driven DW dynamic [11, 12, 28]. Therefore, DW motion induced by transverse current and magnetic field presents common universal dynamical behaviors.

Roughness exponent. In order to discuss this issue from an independent measurement, we have investigated the DW roughness in the creep regime. The DW self affinity was tested using the displacement-displacement correlation function [4]:

$$w(L) = \sum_x [u(x+L) - u(x)]^2, \quad (2)$$

where $u(x)$ is the DW displacement measured parallel to current and L the length of DW segment along the axis x transverse to current (see the inset of Fig. 4 (A)). For a self-affine interface ($u(L) \sim L^\zeta$), the function $w(L)$ is expected to follow a power law variation $w(L) \sim L^{2\zeta}$, where ζ is the roughness exponent. Typical variations of $w(L)$ versus L obtained for field and current induced motion are compared in Fig. 4 (B) in log-log scale. As it can be observed, above the microscope resolution ($\approx 1 \mu m$), both curves present a linear variation over the range $L = 1-10 \mu m$ with similar slopes ($= 2\zeta$). In order to get a more quantitative comparison, the slope of linear fits were systematically measured for successions of DW positions (as shown in Fig.1) and a temperature varying over one decade ($T = 4.5-59 K$). No significant variation of ζ_j was observed with DW tilting (see Ref. [25] for details) and ζ_j remained always smaller than the value ($\zeta_j = 0.99 \pm 0.01$) reported in Ref. [5]. This is most probably associated to a much lower DW tilting observed for (Ga,Mn)(As,P) than for Pt/Co/Pt. The mean and standard deviation of the roughness exponent for current (ζ_j) and field (ζ_H) driven DW motion is reported in Fig. 4 as a function of temperature. As expected for universal

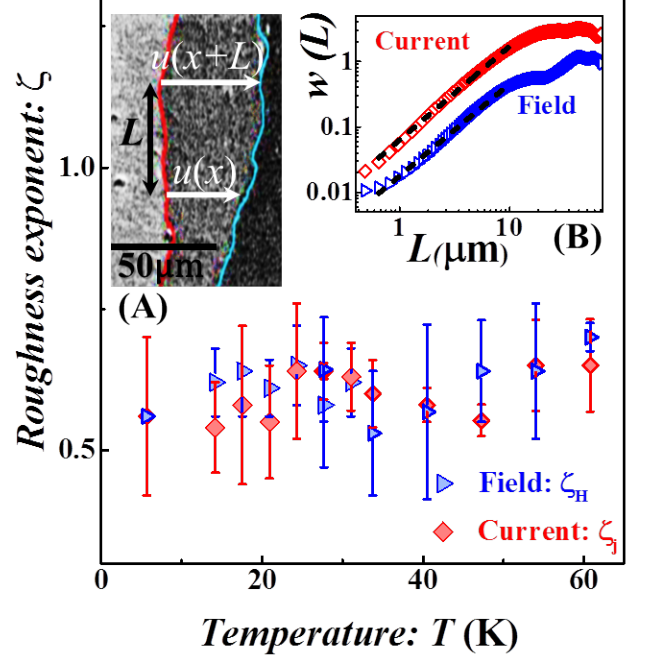


Figure 4. **Analysis of domain wall roughness.** Roughness exponents ζ_j and ζ_H as a function of temperature, measured for $j < j_d$ and $H < H_d$, respectively (see [25]). Inset (A): Definition of the domain wall displacements $u(x)$ and $u(x+L)$ used to calculate the displacement-displacement correlation function (see Eq. 2). Inset (B): Typical correlation functions w versus DW segment length L in log-log scale, for current (diamonds) and field (triangles) driven DW ($T = 14.2 K$). The dashed lines are fit of $w \sim L^{2\zeta}$ used to determine the roughness exponents ζ_j and ζ_H .

critical exponents, the values of ζ_j and ζ_H do not vary significantly. Their mean values ($\zeta_j = 0.60 \pm 0.05$ and $\zeta_H = 0.61 \pm 0.04$), calculated from all measurements, agree well within experimental error. Both are compatible with the value ($\zeta_j = 0.68 \pm 0.04$ [5]) obtained by Moon *et al.* [5] for a DW roughness analyzed in the direction (\vec{n}) normal to DW and with usual experimental results reported in the literature for field driven DW motion [4, 5, 9]. A good agreement is also obtained with theoretical predictions ($\zeta = 0.635 \pm 0.005$) [21, 29] for the universality class of the qEW model with short range disorder and elasticity including an-harmonic correction.

The common universal behaviors observed both for the roughness and dynamics of field and current driven DW motion seems *a priori* surprising since no faceting of DW is expected for the qEW universality class. This apparent paradox can be explained from the variation of driving force with DW tilting discussed at the beginning of the letter. Along $-\vec{j}$, the magnitude of driving force is proportional to the product $j \cos \theta$. The second order expansion of $\cos \theta$ ($\approx 1 - (1/2)(\partial u / \partial x)^2$), introduces a

term in the equation of motion similar to the so-called KPZ term producing interface tilting: $\lambda(\partial u/\partial x)^2$, with $\lambda = -j/2$ [26]. However, in the direction \vec{n} perpendicular to DW, the driving force is simply proportional to the current density ($f \propto j$) and acts as a magnetic field ($f \propto H$), which explains a compatibility with the qEW universality class.

In conclusion, the common universal behaviors with field driven DW motion and in particular the compatibility with the self-consistent description of creep and depinning regimes could help to better understand current induced DW motion experiments [2] since it allows a clear identification of dynamical regimes and to discriminate universal from material dependent behaviors [28]. It would be also very interesting to study the universal behaviors of DWs driven by spin-orbit-torque [30] and of DWs in antiferromagnets [31]. Moreover, the instability of transverse alignment between DW and current should have direct implications for potential applications based on the controlled motion of DWs [1] in nanowires.

We wish to thank S. Bustingorry, A. Kolton, and K. Wiese for fruitful discussions. This work was partly supported by the projects DIM CNano IdF (Region Ile-de-France) and the Labex NanoSaclay (ANR-10-LABX-0035). R.D.P. thanks the Mexican council CONACyT for the PhD fellowship n0: 449563.

* vincent.jeudy@u-psud.fr

- [1] S. S. P. Parkin and S.-H. Yang, Nature Nanotechnology **10**, 195 (2015).
- [2] L. Caretta, M. Mann, F. Büttner, K. Ueda, B. Pfau, C. M. Günther, P. Hessler, A. Churikova, C. Klose, M. Schneider, D. Engel, C. Marcus, D. Bono, K. Bagschik, S. Eisebitt, and G. S. D. Beach, Nature Nanotechnology, 1 (2018).
- [3] A. Hrabec, K. Shahbazi, T. A. Moore, E. Martinez, and C. H. Marrows, Nanotechnology **30**, 234003 (2019).
- [4] S. Lemerle, J. Ferré, C. Chappert, V. Mathet, T. Giamarchi, and P. Le Doussal, Phys. Rev. Lett. **80**, 849 (1998).
- [5] K.-W. Moon, D.-H. Kim, S.-C. Yoo, C.-G. Cho, S. Hwang, B. Kahng, B.-C. Min, K.-H. Shin, and S.-B. Choe, Phys. Rev. Lett. **110**, 107203 (2013).
- [6] E. E. Ferrero, L. Foini, T. Giamarchi, A. B. Kolton, and A. Rosso, Phys. Rev. Lett. **118**, 147208 (2017).
- [7] M. P. Grassi, A. B. Kolton, V. Jeudy, A. Mougin, S. Bustingorry, and J. Curiale, Phys. Rev. B **98**, 224201 (2018).
- [8] M. Yamanouchi, J. Ieda, F. Matsukura, S. E. Barnes, S. Maekawa, and H. Ohno, Science **317**, 1726 (2007).
- [9] P. J. Metaxas, J. P. Jamet, A. Mougin, M. Cormier, J. Ferré, V. Baltz, B. Rodmacq, B. Dieny, and R. L. Stamps, Phys. Rev. Lett. **99**, 217208 (2007).
- [10] S. DuttaGupta, S. Fukami, C. Zhang, H. Sato, M. Yamanouchi, F. Matsukura, and H. Ohno, Nature Physics **12**, 333 (2016).
- [11] V. Jeudy, A. Mougin, S. Bustingorry, W. Savero Torres, J. Gorchon, A. B. Kolton, A. Lemaître, and J.-P. Jamet, Phys. Rev. Lett. **117**, 057201 (2016).
- [12] R. Diaz Pardo, W. Savero Torres, A. B. Kolton, S. Bustingorry, and V. Jeudy, Phys. Rev. B **95**, 184434 (2017).
- [13] S. Atis, A. K. Dubey, D. Salin, L. Talon, P. Le Doussal, and K. J. Wiese, Phys. Rev. Lett. **114**, 234502 (2015).
- [14] J. A. Bonachela, C. D. Nadell, J. B. Xavier, and S. A. Levin, Journal of Statistical Physics **144**, 303 (2011).
- [15] S. Moulinet, C. Guthmann, and E. Rolley, The European Physical Journal E **8**, 437 (2002).
- [16] T. Tybell, P. Paruch, T. Giamarchi, and J.-M. Triscone, Phys. Rev. Lett. **89**, 097601 (2002).
- [17] P. Chauve, T. Giamarchi, and P. Le Doussal, Phys. Rev. B **62**, 6241 (2000).
- [18] P. Le Doussal and K. J. Wiese, Physical Review E - Statistical, Nonlinear, and Soft Matter Physics **79** (2009), 0808.3217.
- [19] S. Bustingorry, A. B. Kolton, and T. Giamarchi, Phys. Rev. E **85**, 021144 (2012).
- [20] A. Rosso and W. Krauth, Phys. Rev. Lett. **87**, 187002 (2001).
- [21] A. B. Kolton, A. Rosso, T. Giamarchi, and W. Krauth, Phys. Rev. B **79**, 184207 (2009).
- [22] J.-C. Lee, K.-J. Kim, J. Ryu, K.-W. Moon, S.-J. Yun, G.-H. Gim, K.-S. Lee, K.-H. Shin, H.-W. Lee, and S.-B. Choe, Phys. Rev. Lett. **107**, 067201 (2011).
- [23] K.-W. Moon, C. Kim, J. Yoon, J. W. Choi, D.-O. Kim, K. M. Song, D. Kim, B. S. Chun, and C. Hwang, Nature Communications **9**, 3788 (2018).
- [24] T. Niazzi, M. Cormier, D. Lucot, L. Largeau, V. Jeudy, J. Cibert, and A. Lemaître, Applied Physics Letters **102**, 122403 (2013).
- [25] See Supplemental Material at <http://link.aps.org/supplemental/...> for details on the sample, Joule heating studies, measurements of velocity and roughness exponent..
- [26] M. Kardar, G. Parisi, and Y.-C. Zhang, Physical Review Letters **56**, 889 (1986).
- [27] The largest values reported in Refs. 8 and 10 could not be reproduced. See also Ref. [11] for discussion on (Ga,Mn)As.
- [28] V. Jeudy, R. Díaz Pardo, W. Savero Torres, S. Bustingorry, and A. B. Kolton, Phys. Rev. B **98**, 054406 (2018).
- [29] A. Rosso, A. K. Hartmann, and W. Krauth, Phys. Rev. E **67**, 021602 (2003).
- [30] E. Martinez, S. Emori, and G. S. D. Beach, Applied Physics Letters **103**, 072406 (2013).
- [31] S.-H. Yang, K.-S. Ryu, and S. Parkin, Nature Nanotechnology **10**, 221 (2015).